Operator Evolution & Factorization in the SRG

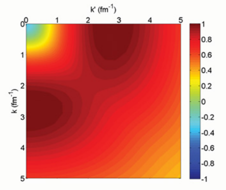

Eric R. Anderson

Department of Physics
& Astronomy
University of North Carolina

November 9, 2012

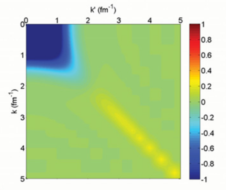

In Collaboration with: S.K Bogner,
R.J. Furnstahl, K. Hebeler,
H. Hergert, & R.J. Perry

Work supported by NSF and UNEDF/SciDAC (DOE)

Outline

1. Overview
   - Resolution & Probes of the Nuclear Wave Function
   - SRG
2. Operator Evolution
   - Properties
   - Many-Body
   - Perturbative Calculation of SRCs
3. Factorization in the SRG
   - Principles
   - Applications
4. Conclusions

Outline

Resolution Scales of Nuclear Physics

Nuclear DFT

⇑

Nuclear Matter

⇑

V_{srg}
NN···N

⇑

Chiral EFT
NN···N

⇑

Lattice QCD

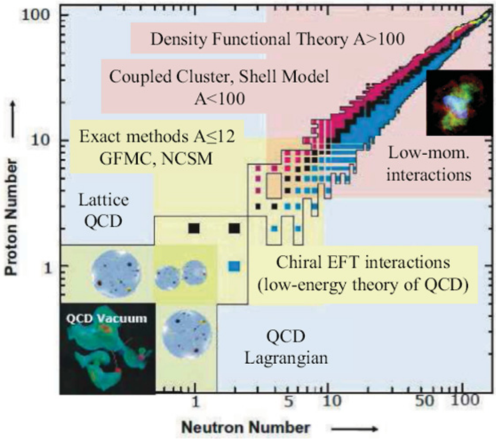

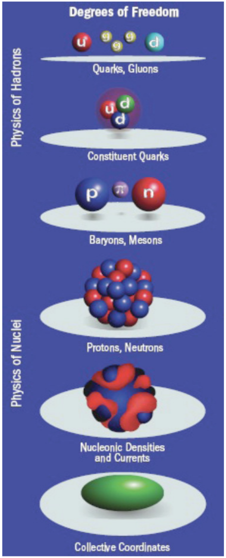

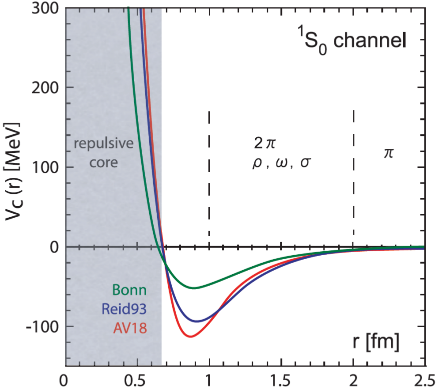

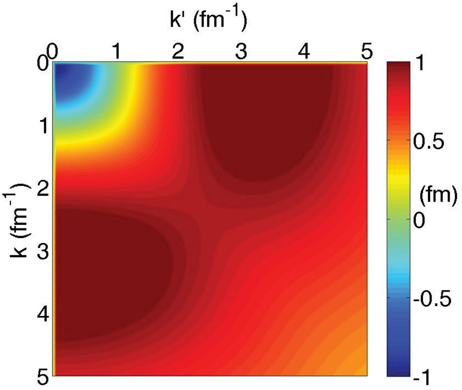

- Typical scale of separation between low- and high-momentum regime in the nuclear wave function at roughly $k_f \approx 250 MeV$

Correlations & Factorization in Nuclear Systems

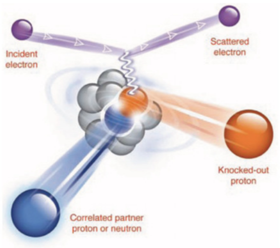

Subedi et al., Science 320,1476 (2008)

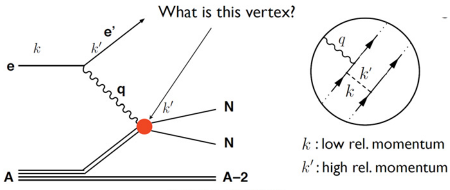

Higinbotham, arXiv:1010.4433

- How is vertex modified?

- E.g.: Detection of knocked out pairs with large relative momenta

- Standard Nuclear physics approach

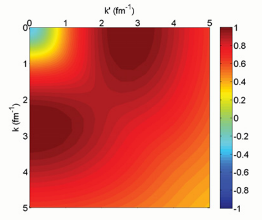

Egiyan et. al, (2006)

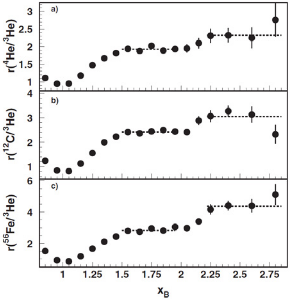

$1.4 \leq Q^2 \leq 2.6\,\text{GeV}^2$

Nucleon Momentum Distributions

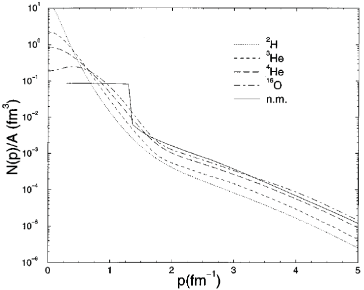

From Pieper, Wiringa, and Pandharipande (1992).

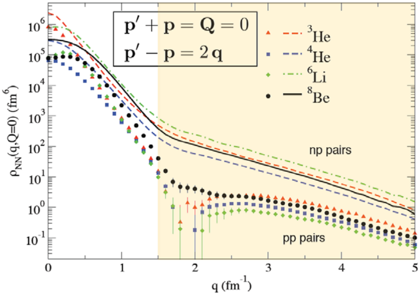

Schiavilla et al., PRL 98, 132501 (2007)

- Scaling behavior of momentum distribution function at large q

$$n_A(k) = a_2(A,d) \cdot n_d(k) \qquad \text{for } k > k_{Fermi}$$

– explained by dominance of NN potential & short-range correlations

- Dominance of *np* pairs over *pp* pairs: explained by tensor forces
- Hard interactions used (high resolution) . . . difficult calculations

Traditional Interpretation

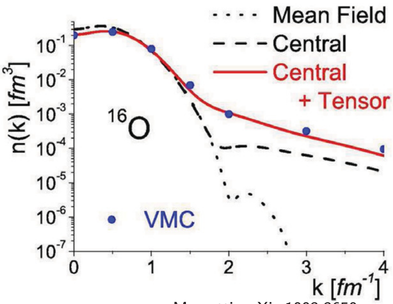

Mezzetti, arXiv:1003.3650.

- Mean field results not sufficient $\Rightarrow$ Introduce SRCs into interaction and wave function
- Factorization of the wave function in this approach

$$\Psi_A(\{\mathbf{p}_i\}_A) \sim [\phi(\mathbf{p}_{rel})\otimes\phi(\mathbf{p}_{CM})]\otimes\Psi_{A-2}(\{\mathbf{p}_i\}_{A-2})$$

- For large $\mathbf{p}_{rel}$, small $\mathbf{p}_{CM}$ $\Rightarrow$ factorization into a 2-particle cluster with high relative momentum and a remaining (A-2)-particle cluster

  $\Rightarrow$ Dominance of 2-body interactions

  - Advantage: Simple operator, $a^\dagger a$
  - Disadvantages:
    – Highly correlated interaction and wave function $\rightarrow$ Difficult to compute!
    – Resolution scale not appropriate for nucleonic dof's

- Alternative factorization of the wave function at high-momentum $\mathbf{q}$ above a decoupling scale λ

$$\Psi_\alpha^\infty(q) \approx \gamma^\lambda(q)\int_0^\lambda p^2 dp\; Z(\lambda)\Psi_\alpha^\lambda(p)$$

– state-independent $\gamma(\mathbf{q})$ and
– state-dependent integral over low momentum

$\longrightarrow$ Wave function easy to calculate $\Rightarrow$ Short-distance physics described by operators!

$\longrightarrow$First need to address strong coupling in Hamiltonian . . .

The Nuclear Interaction

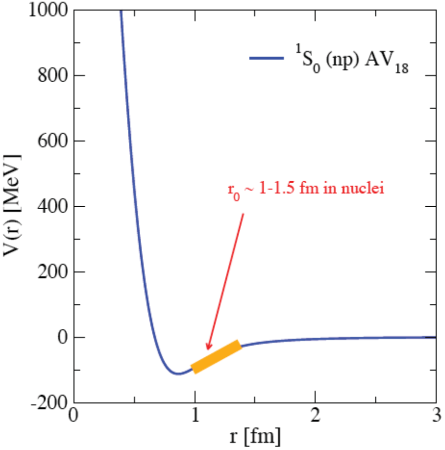

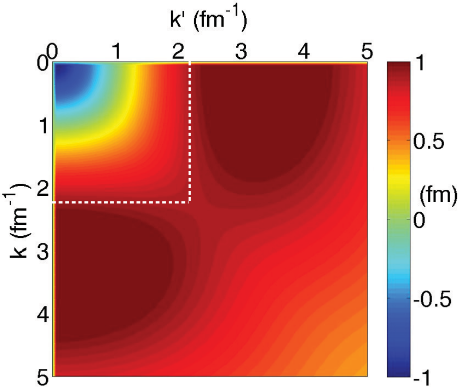

- High momentum matrix elements lead to computationally infeasible many-body problem for all but lightest nuclei

Growth of Configuration interaction matrices

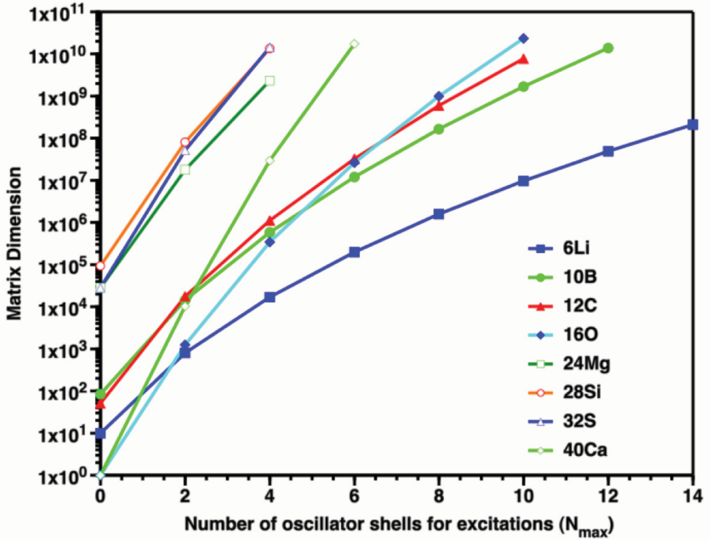

Introduction to the SRG: Potentials

- **The Similarity Renormalization Group (SRG)**

  → provides a means to systematically evolve computationally difficult Hamiltonians toward diagonal or decoupled form

  → simplifies calculations with nuclear potentials

- Based on unitary transformations as shown here:

$$H_s = U_s H_{s=0} U_s^\dagger \equiv T_{\rm rel} + V_s$$

→ Differentiating with respect to s gives the *flow equation*:

$$\frac{dH_s}{ds} = [\eta_s, H_s] \quad \text{where} \quad \eta_s = \frac{dU_s}{ds} U_s^\dagger = -\eta_s^\dagger$$

  – The flow can be specified in η_s by a flow operator G_s:

$$\eta_s = [G_s, H_s]$$

  – Typically:

$$G_s = T_{\rm rel} \implies \frac{dH_s}{ds} = [[T_{\rm rel}, H_s], H_s]$$

Flow equations in action: NN only

- In each partial wave with $\epsilon_k = \hbar^2 k^2/M$ and $\lambda = 1/s^{1/4}$ fm^{-1}

$$\frac{dV_\lambda}{d\lambda}(k,k') \propto -(\epsilon_k - \epsilon_{k'})^2 V_\lambda(k,k') + \sum_q (\epsilon_k + \epsilon_{k'} - 2\epsilon_q) V_\lambda(k,q) V_\lambda(q,k')$$

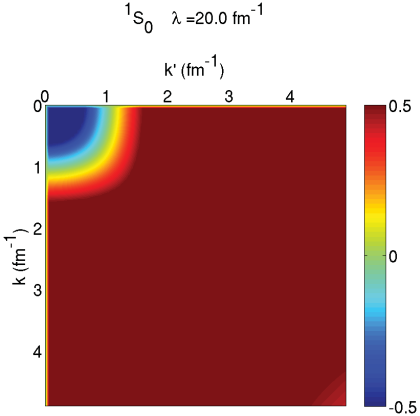

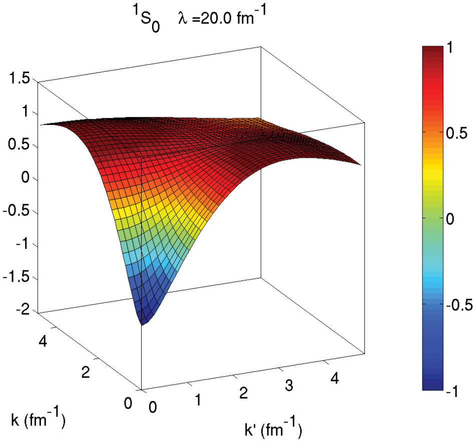

Flow equations in action: NN only

- In each partial wave with $\epsilon_k = \hbar^2 k^2/M$ and $\lambda = 1/s^{1/4}\ \text{fm}^{-1}$

$$\frac{dV_\lambda}{d\lambda}(k,k') \propto -(\epsilon_k - \epsilon_{k'})^2 V_\lambda(k,k') + \sum_q (\epsilon_k + \epsilon_{k'} - 2\epsilon_q) V_\lambda(k,q) V_\lambda(q,k')$$

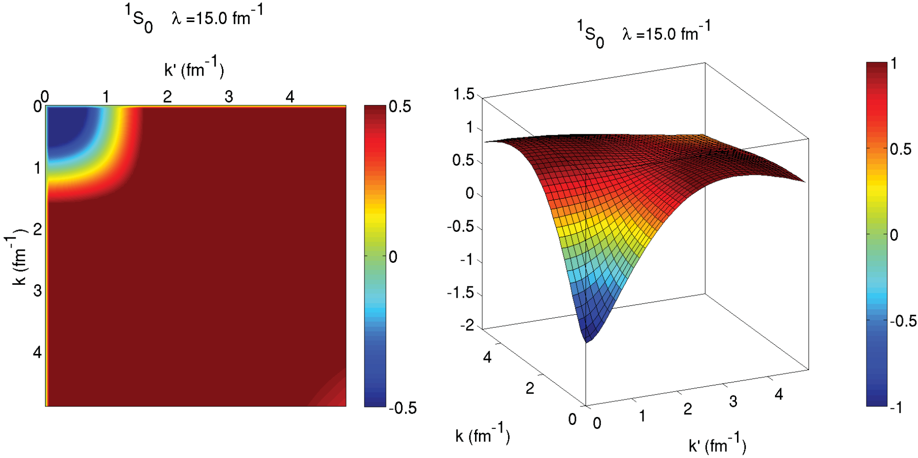

Flow equations in action: NN only

- In each partial wave with $\epsilon_k = \hbar^2 k^2/M$ and $\lambda = 1/s^{1/4}$ fm^{-1}

$$\frac{dV_\lambda}{d\lambda}(k,k') \propto -(\epsilon_k - \epsilon_{k'})^2 V_\lambda(k,k') + \sum_q (\epsilon_k + \epsilon_{k'} - 2\epsilon_q) V_\lambda(k,q) V_\lambda(q,k')$$

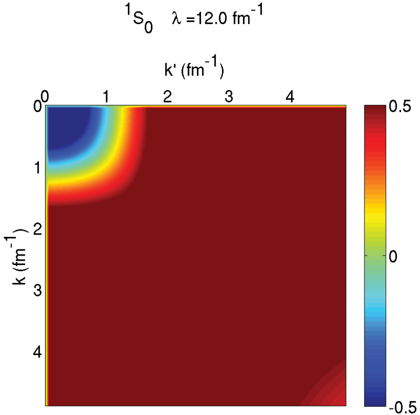

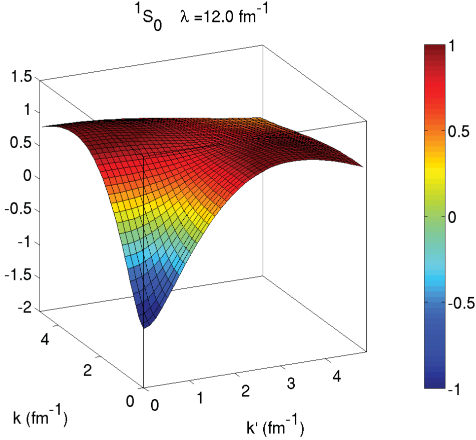

Flow equations in action: NN only

- In each partial wave with $\epsilon_k = \hbar^2 k^2/M$ and $\lambda = 1/s^{1/4}\ \mathrm{fm}^{-1}$

$$\frac{dV_\lambda}{d\lambda}(k,k') \propto -(\epsilon_k - \epsilon_{k'})^2 V_\lambda(k,k') + \sum_q (\epsilon_k + \epsilon_{k'} - 2\epsilon_q) V_\lambda(k,q) V_\lambda(q,k')$$

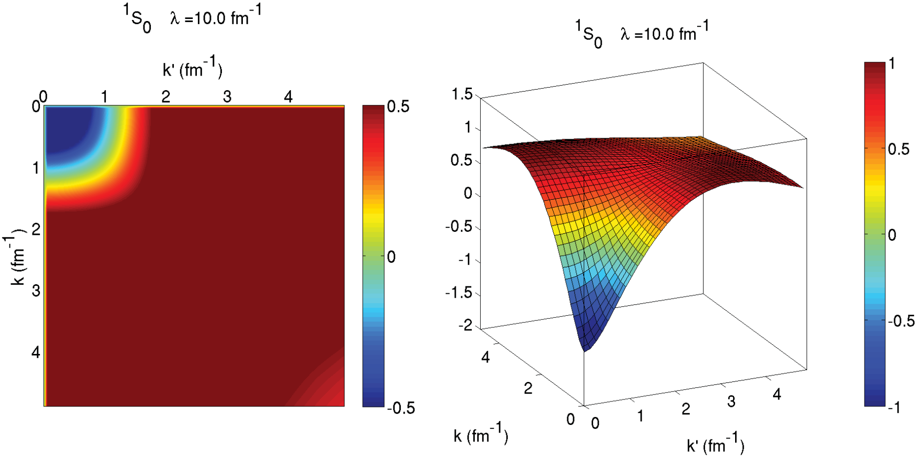

Flow equations in action: NN only

- In each partial wave with $\epsilon_k = \hbar^2 k^2/M$ and $\lambda = 1/s^{1/4}\ \text{fm}^{-1}$

$$\frac{dV_\lambda}{d\lambda}(k,k') \propto -(\epsilon_k - \epsilon_{k'})^2 V_\lambda(k,k') + \sum_q (\epsilon_k + \epsilon_{k'} - 2\epsilon_q) V_\lambda(k,q) V_\lambda(q,k')$$

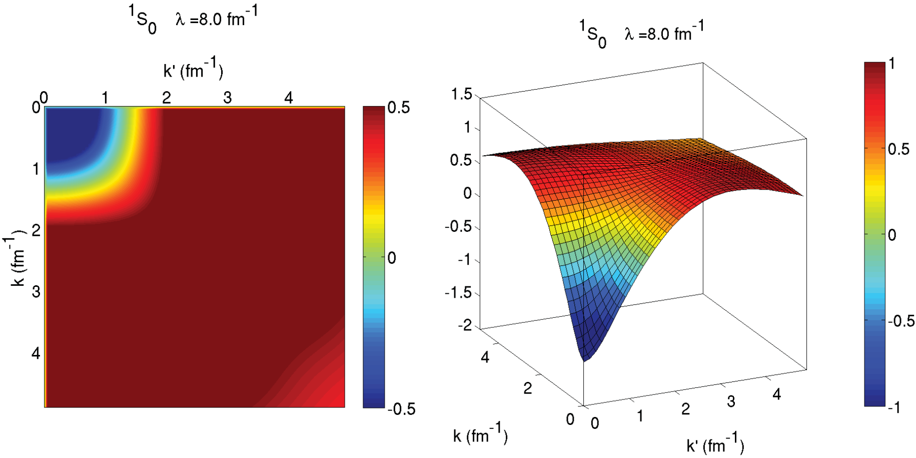

Flow equations in action: NN only

- In each partial wave with $\epsilon_k = \hbar^2 k^2/M$ and $\lambda = 1/s^{1/4}\ \text{fm}^{-1}$

$$\frac{dV_\lambda}{d\lambda}(k,k') \propto -(\epsilon_k - \epsilon_{k'})^2 V_\lambda(k,k') + \sum_q (\epsilon_k + \epsilon_{k'} - 2\epsilon_q) V_\lambda(k,q) V_\lambda(q,k')$$

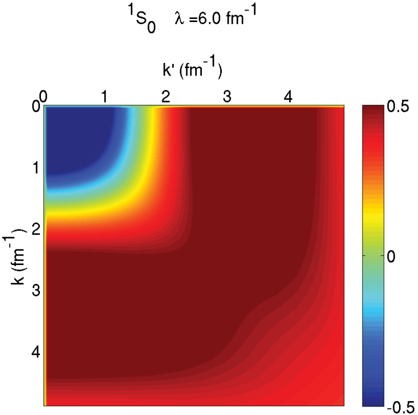

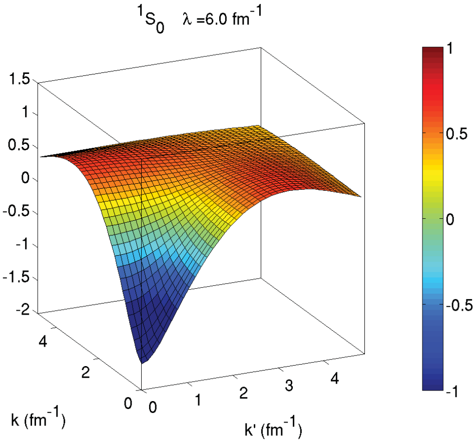

Flow equations in action: NN only

- In each partial wave with $\epsilon_k = \hbar^2 k^2/M$ and $\lambda = 1/s^{1/4}\ \text{fm}^{-1}$

$$\frac{dV_\lambda}{d\lambda}(k,k') \propto -(\epsilon_k - \epsilon_{k'})^2 V_\lambda(k,k') + \sum_q (\epsilon_k + \epsilon_{k'} - 2\epsilon_q) V_\lambda(k,q) V_\lambda(q,k')$$

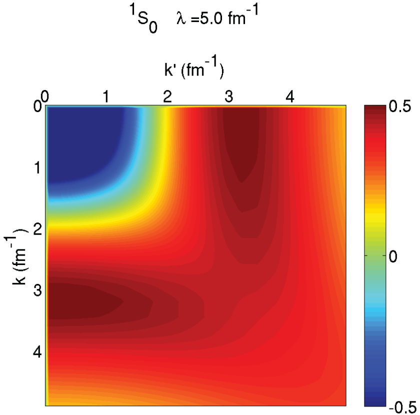

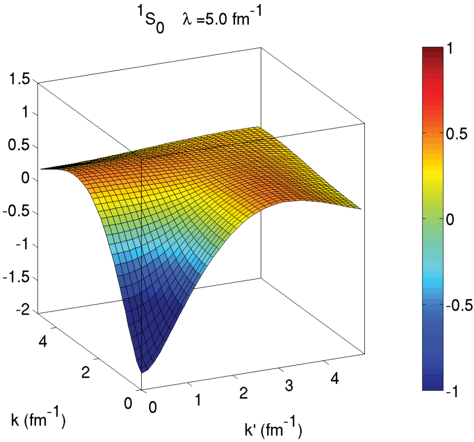

Flow equations in action: NN only

- In each partial wave with $\epsilon_k = \hbar^2 k^2/M$ and $\lambda = 1/s^{1/4}\ \mathrm{fm}^{-1}$

$$\frac{dV_\lambda}{d\lambda}(k,k') \propto -(\epsilon_k - \epsilon_{k'})^2 V_\lambda(k,k') + \sum_q (\epsilon_k + \epsilon_{k'} - 2\epsilon_q) V_\lambda(k,q) V_\lambda(q,k')$$

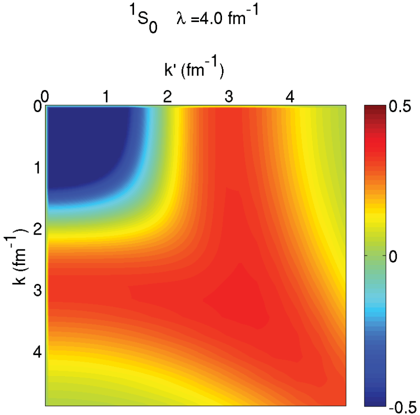

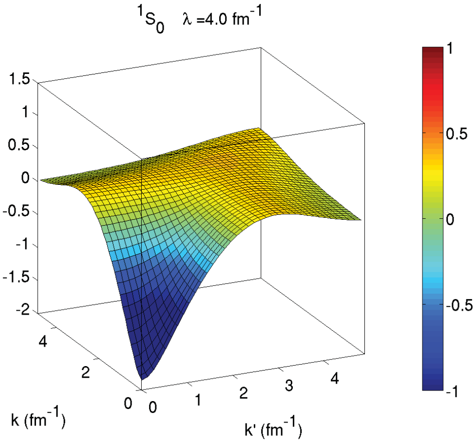

- In each partial wave with $\epsilon_k = \hbar^2 k^2/M$ and $\lambda = 1/s^{1/4}\ \mathrm{fm}^{-1}$

$$\frac{dV_\lambda}{d\lambda}(k,k') \propto -(\epsilon_k - \epsilon_{k'})^2 V_\lambda(k,k') + \sum_q (\epsilon_k + \epsilon_{k'} - 2\epsilon_q) V_\lambda(k,q) V_\lambda(q,k')$$

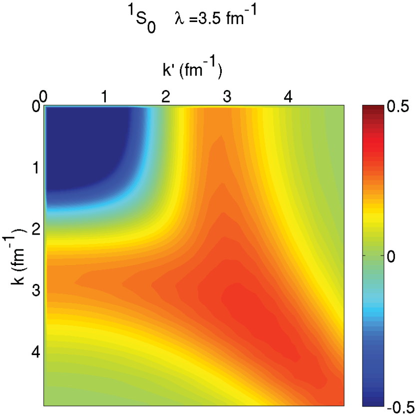

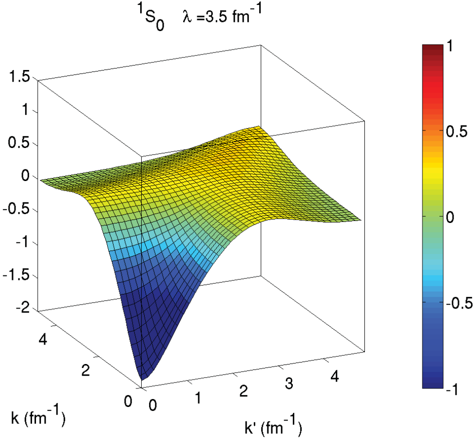

Flow equations in action: NN only

- In each partial wave with $\epsilon_k = \hbar^2 k^2 / M$ and $\lambda = 1/s^{1/4}\ \text{fm}^{-1}$

$$\frac{dV_\lambda}{d\lambda}(k,k') \propto -(\epsilon_k - \epsilon_{k'})^2 V_\lambda(k,k') + \sum_q (\epsilon_k + \epsilon_{k'} - 2\epsilon_q) V_\lambda(k,q) V_\lambda(q,k')$$

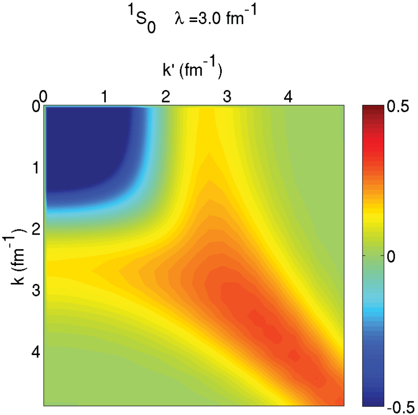

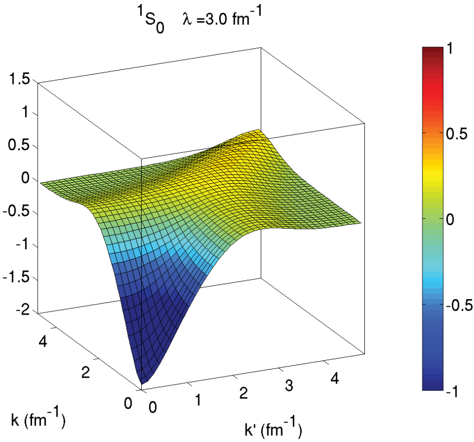

Flow equations in action: NN only

- In each partial wave with $\epsilon_k = \hbar^2 k^2/M$ and $\lambda = 1/s^{1/4}\ \mathrm{fm}^{-1}$

$$\frac{dV_\lambda}{d\lambda}(k,k') \propto -(\epsilon_k - \epsilon_{k'})^2 V_\lambda(k,k') + \sum_q (\epsilon_k + \epsilon_{k'} - 2\epsilon_q) V_\lambda(k,q) V_\lambda(q,k')$$

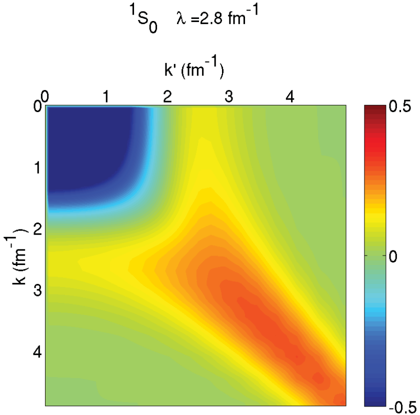

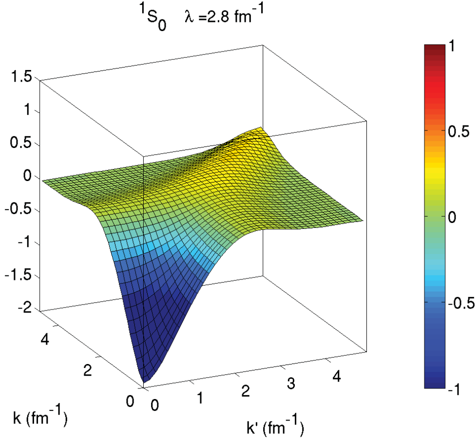

Flow equations in action: NN only

- In each partial wave with $\epsilon_k = \hbar^2 k^2/M$ and $\lambda = 1/s^{1/4}\ \text{fm}^{-1}$

$$\frac{dV_\lambda}{d\lambda}(k,k') \propto -(\epsilon_k - \epsilon_{k'})^2 V_\lambda(k,k') + \sum_q (\epsilon_k + \epsilon_{k'} - 2\epsilon_q) V_\lambda(k,q) V_\lambda(q,k')$$

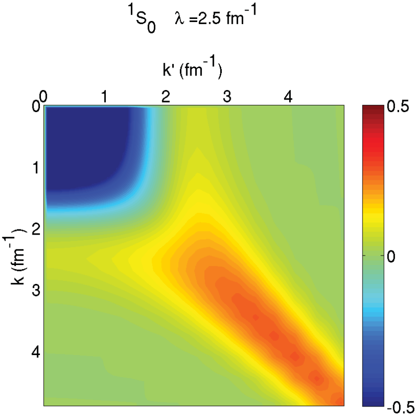

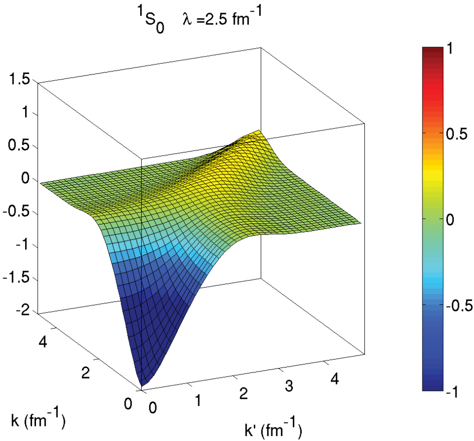

Flow equations in action: NN only

- In each partial wave with $\epsilon_k = \hbar^2 k^2/M$ and $\lambda = 1/s^{1/4}\ \text{fm}^{-1}$

$$\frac{dV_\lambda}{d\lambda}(k,k') \propto -(\epsilon_k - \epsilon_{k'})^2 V_\lambda(k,k') + \sum_q (\epsilon_k + \epsilon_{k'} - 2\epsilon_q) V_\lambda(k,q) V_\lambda(q,k')$$

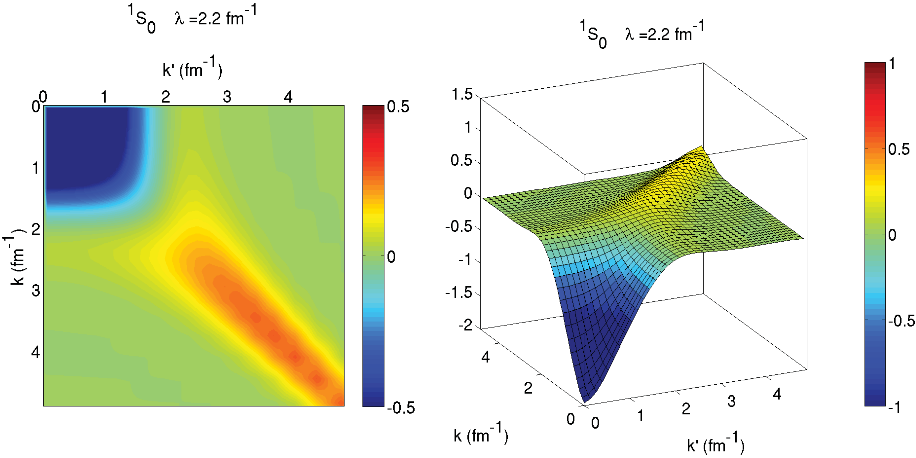

Flow equations in action: NN only

- In each partial wave with $\epsilon_k = \hbar^2 k^2/M$ and $\lambda = 1/s^{1/4}\ \mathrm{fm}^{-1}$

$$\frac{dV_\lambda}{d\lambda}(k,k') \propto -(\epsilon_k - \epsilon_{k'})^2 V_\lambda(k,k') + \sum_q (\epsilon_k + \epsilon_{k'} - 2\epsilon_q) V_\lambda(k,q) V_\lambda(q,k')$$

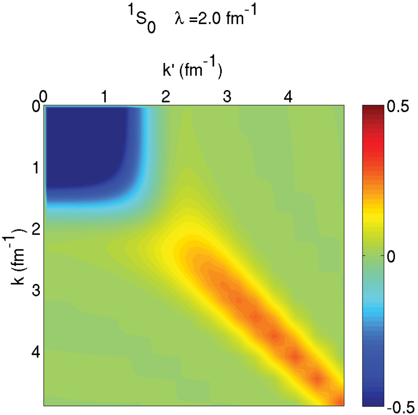

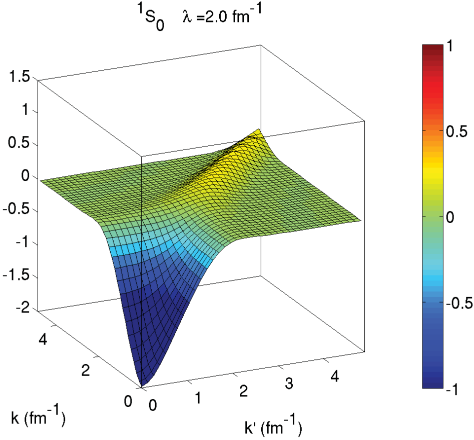

NCSM Calculations for Light Nuclei

- Harmonic oscillator basis with $N_{\max}$ shells for excitations
- Graphs show convergence for *soft* chiral EFT potential and evolved SRG potentials (including NNN)

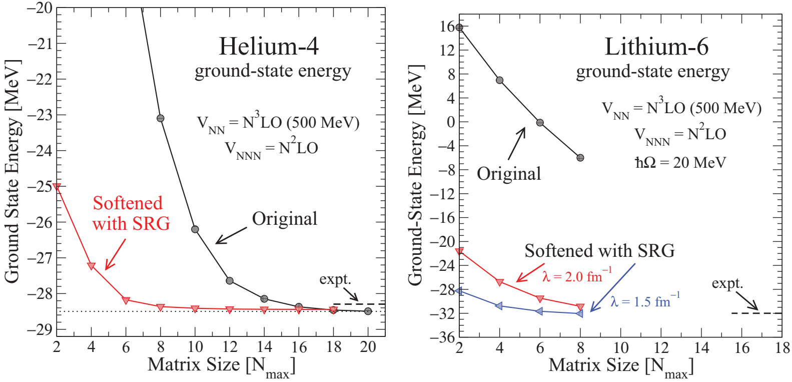

[E. Jurgenson, P. Navrátil, R.J. Furnstahl (PRC, 2011)]

- Better convergence, but rapid growth of basis still a problem (solution: importance sampling of matrix elements [R. Roth])

Hierarchy of Many-Body Effects with $T_{\rm rel}$ SRG Evolution

- Consider a's and $a^\dagger$'s wrt s.p. basis and reference state:

$$\frac{dV_s}{ds} = \Big[\Big[\sum \underbrace{a^\dagger a}_{G_s}, \sum \underbrace{a^\dagger a^\dagger a a}_{\text{2-body}}\Big], \sum \underbrace{a^\dagger a^\dagger a a}_{\text{2-body}}\Big] = \cdots + \sum \underbrace{a^\dagger a^\dagger a^\dagger a a a}_{\text{3-body!}} + \cdots$$

  so there will be A-body forces (and operators) generated

- Compare 2-body only to full $2+3$-body evolution:

  [E. Jurgenson, P. Navrátil, R.J. Furnstahl (PRC, 2011)]

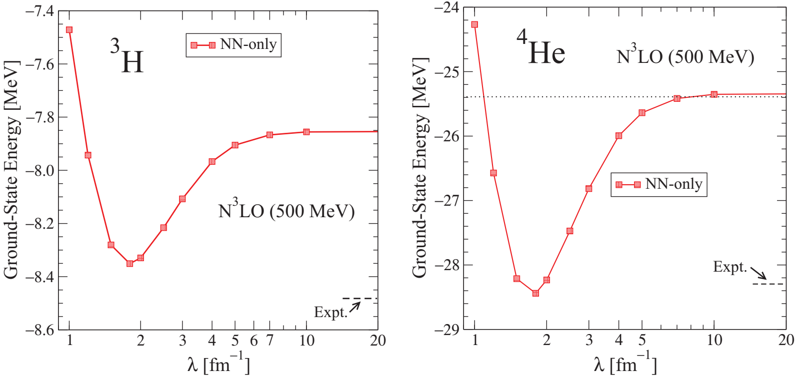

Hierarchy of Many-Body Effects with $T_{\rm rel}$ SRG Evolution

- Consider a's and $a^\dagger$'s wrt s.p. basis and reference state:

$$\frac{dV_s}{ds} = \Big[\Big[\sum \underbrace{a^\dagger a}_{G_s}, \sum \underbrace{a^\dagger a^\dagger a a}_{\text{2-body}}\Big], \sum \underbrace{a^\dagger a^\dagger a a}_{\text{2-body}}\Big] = \cdots + \sum \underbrace{a^\dagger a^\dagger a^\dagger a a a}_{\text{3-body!}} + \cdots$$

so there will be A-body forces (and operators) generated

- Compare 2-body only to full $2 + 3$-body evolution:

[E. Jurgenson, P. Navrátil, R.J. Furnstahl (PRC, 2011)]

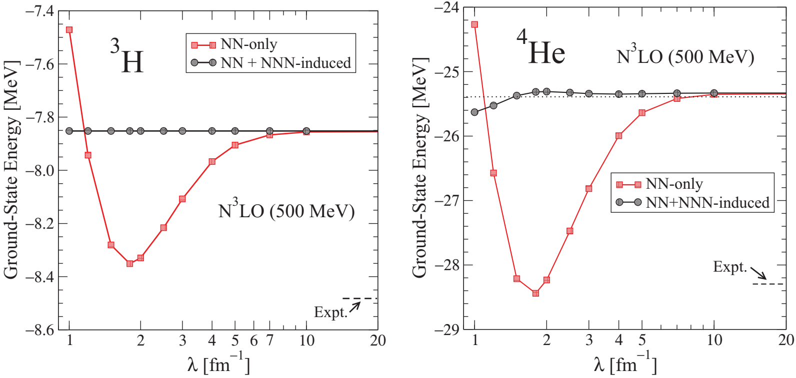

Hierarchy of Many-Body Effects with $T_{\rm rel}$ SRG Evolution

- Consider a's and $a^\dagger$'s wrt s.p. basis and reference state:

$$\frac{dV_s}{ds} = \Big[\Big[\underbrace{\sum a^\dagger a}_{G_s}, \underbrace{\sum a^\dagger a^\dagger a a}_{\text{2-body}}\Big], \underbrace{\sum a^\dagger a^\dagger a a}_{\text{2-body}}\Big] = \cdots + \underbrace{\sum a^\dagger a^\dagger a^\dagger a a a}_{\text{3-body!}} + \cdots$$

so there will be A-body forces (and operators) generated

- Compare 2-body only to full 2 + 3-body evolution:

[E. Jurgenson, P. Navrátil, R.J. Furnstahl (PRC, 2011)]

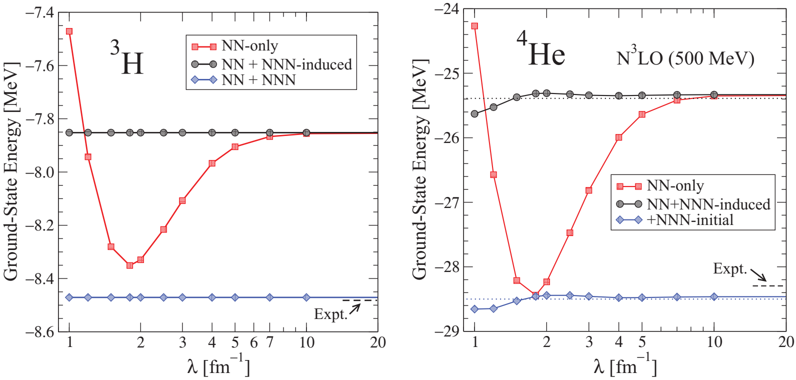

Outline

Introduction to the SRG: Operator Evolution

- Same unitary transformation **evolves potentials and operators!**

$$O_s = U_s O_{s=0} U_s^\dagger \quad \Longleftrightarrow \quad \frac{dO_s}{ds} = [\eta_s, O_s] = [[T_{rel}, H_s], O_s]$$

Can construct transformation directly . . .

$$U_s = \sum_\alpha |\psi_\alpha(s)\rangle \langle \psi_\alpha(0)|$$

$$\Rightarrow U_s(k_i, k_j) = \sum_\alpha \langle k_i|\psi_\alpha(s)\rangle \langle \psi_\alpha(0)|k_j\rangle$$

or, e.g., evolve from DE

$$\frac{dO_s(k,k')}{ds} = \frac{2}{\pi}\int_0^\infty q^2 dq\, [(k^2 - q^2) V_s(k,q) O_s(q,k') + (k'^2 - q^2) O_s(k,q) V_s(q,k')]$$

- Evolve operators consistent with N3LO 500MeV potential
  - $\rightarrow$ Number Operator, RMS radius, Quadrupole moment, $\left\langle \frac{1}{r} \right\rangle$, etc.
  - $\rightarrow$ Observables in deuteron

[era, S.K. Bogner, R.J. Furnstahl, R.J. Perry, (PRC, 2010)]

Deuteron Momentum Distribution

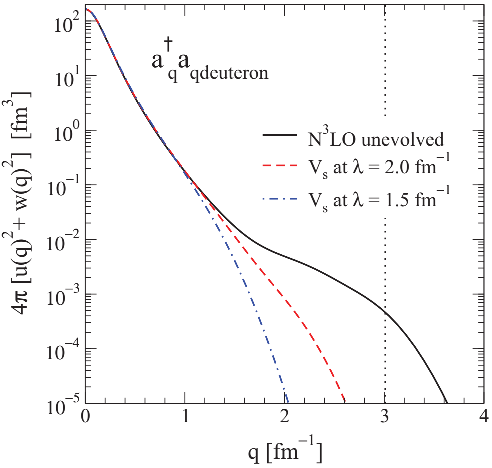

Number Operator - High Momentum

- In **partial wave momentum basis** (for $q = 3.02\,\text{fm}^{-1}$):

Operator:
$\langle k|\, U_\lambda a_q^\dagger a_q U_\lambda^\dagger \,|k'\rangle$

Integrand:
$\langle \psi_d^\lambda|\, U_\lambda a_q^\dagger a_q U_\lambda^\dagger \,|\psi_d^\lambda\rangle$

Integrand on log scale

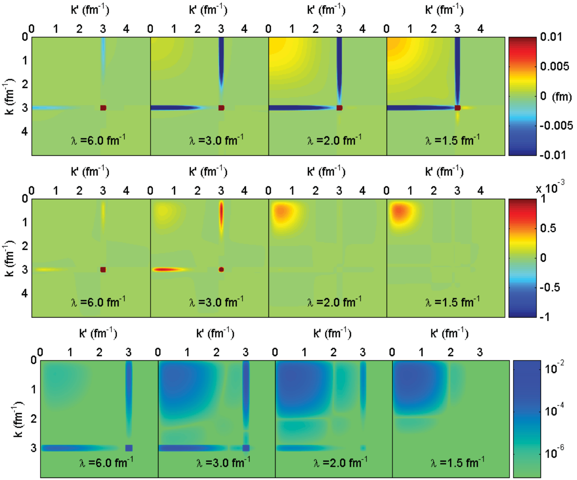

- **Decoupling** $\leftrightarrow$ High momentum components suppressed
- *Integrated value does not change, but nature of operator does*

Deuteron Momentum Distribution

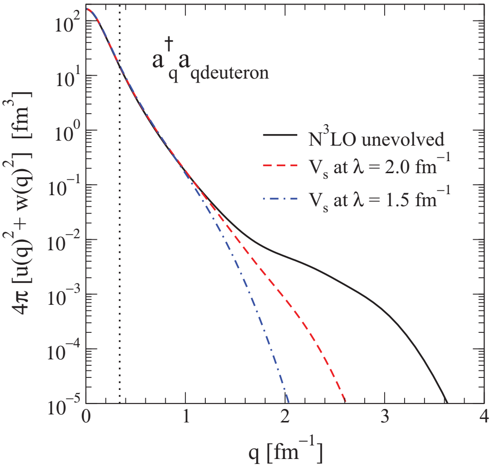

- In **partial wave momentum basis** (for $q = 0.34\,\mathrm{fm}^{-1}$):

Operator:
$\langle k|\, U_\lambda a_q^\dagger a_q U_\lambda^\dagger \,|k'\rangle$

Integrand:
$\langle \psi_d^\lambda|\, U_\lambda a_q^\dagger a_q U_\lambda^\dagger \,|\psi_d^\lambda\rangle$

Integrand on log scale

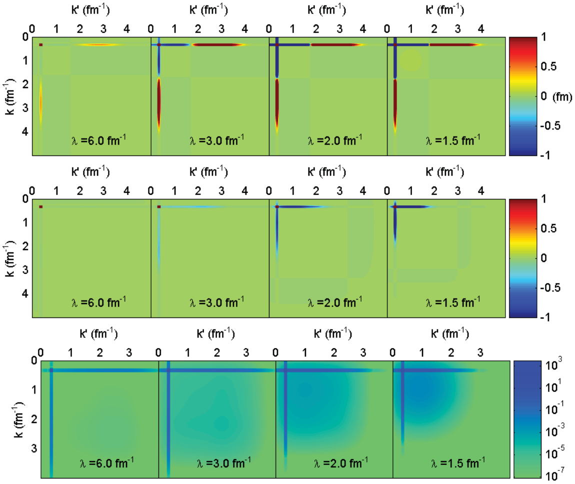

- Strength remains at low momentum
- Similar for other long distance operators: $\langle r^2\rangle$, $\langle Q_d\rangle$, & $\langle \frac{1}{r}\rangle$

Demonstration of Decoupling In Expectation Values

- **Evolve** Hamiltonian **&** operators **to λ in full space $\rightarrow$ TRUNCATE at Λ:**

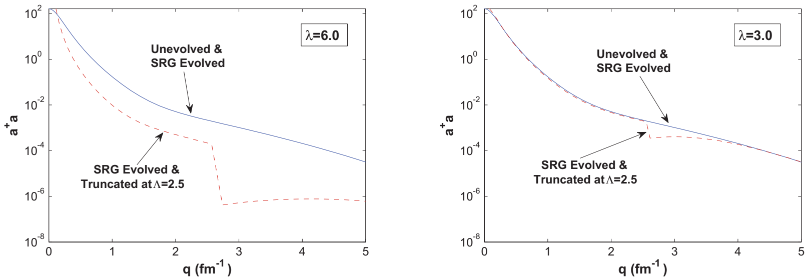

- Momentum distribution
  - Calculated with AV18 potential.
  - $\Lambda = 2.5\,\text{fm}^{-1}$
    $\lambda = 6.0\,\text{fm}^{-1}, 3.0\,\text{fm}^{-1}$, and $2.0\,\text{fm}^{-1}$
- Decoupling **for all q** is successful when $\lambda < \Lambda$

  $\Rightarrow$ Expectation values reproduced in truncated basis

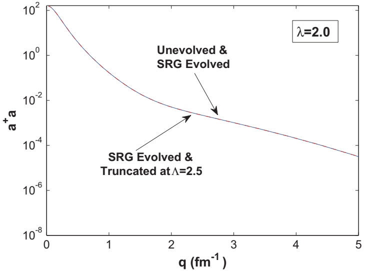

Many-Body evolution of Operators

- **Many-body evolution** with operators normal ordered in the vacuum:

$$\frac{d\widehat{O}_s}{ds} = [[T_{\rm rel}, H_s], \widehat{O}_s] \Longrightarrow \left[\left[\sum_{ij} T_{ij} a_i^\dagger a_j, \sum_{i'j'} T_{i'j'} a_{i'}^\dagger a_{j'} + \frac{1}{2}\sum_{pqkl} V_{pqkl|s} a_p^\dagger a_q^\dagger a_l a_k + \cdots\right], \widehat{O}_s\right]$$

$\rightarrow$ Only one non-vanishing contraction in the vacuum: $\overbracket{a_i a_j^\dagger} = \delta_{ij}$

- A general operator $\widehat{O}$ for an A-body system can be written as

$$\widehat{O} = \widehat{O}^{(1)} + \widehat{O}^{(2)} + \widehat{O}^{(3)} + \cdots + \widehat{O}^{(A)}$$

where the $\widehat{O}^{(i)}$ label the $i = 1, 2, 3, ..., A$-body components
– SRG operator $\widehat{O}_s$ will have contributions for all n so that $\widehat{O}^{(n)} \neq \widehat{O}_s^{(n)}$.

- Expanding commutators and making contractions, one finds:

$\rightarrow$ Evolution of an operator is fixed in each n-particle subspace

$\rightarrow$ For interactions with $n \geq 2$-body components, 1-body component in $\widehat{O}_s$ will have no induced 1-body components

$\rightarrow$ **How do we deal with this in practice?**

Operator Evolution & Extraction Process

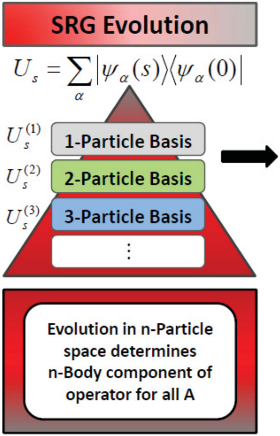

Operator Evolution & Extraction Process

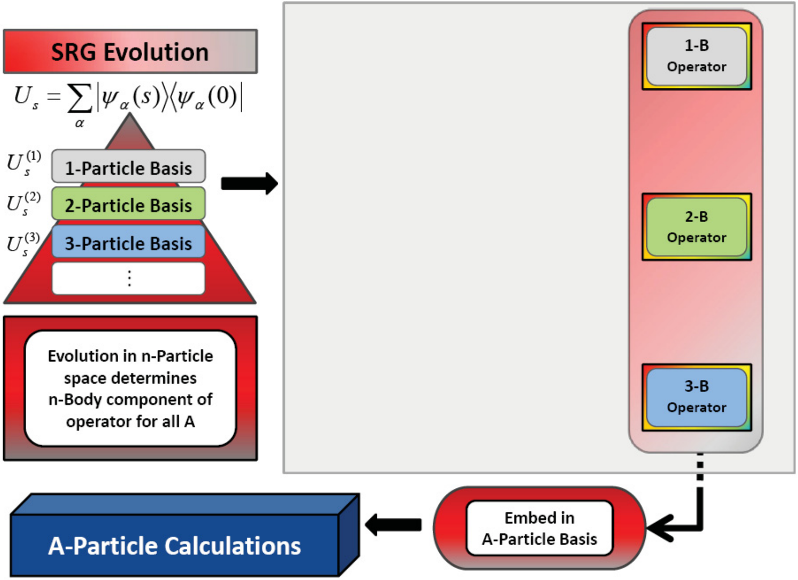

Operator Evolution & Extraction Process

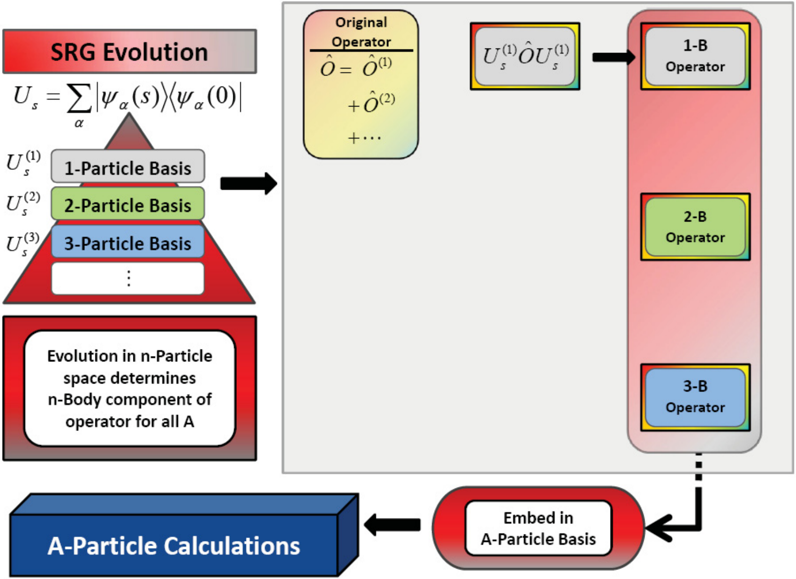

Operator Evolution & Extraction Process

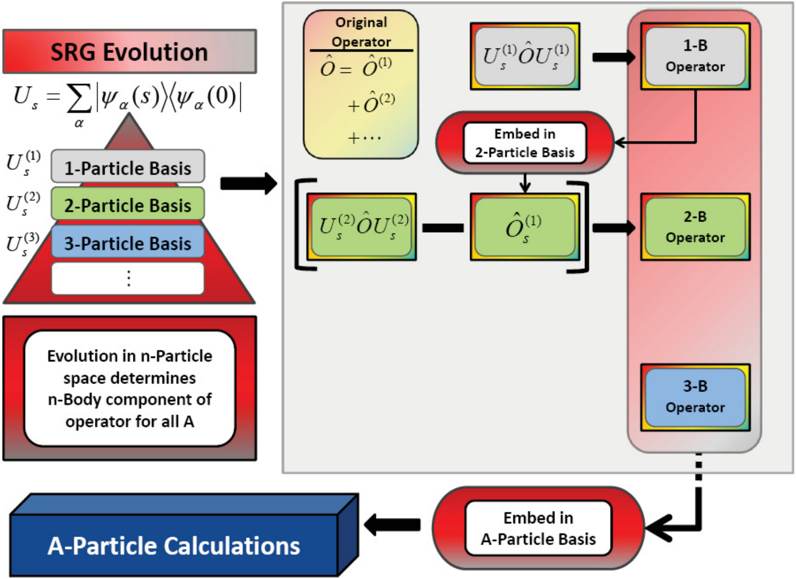

Operator Evolution & Extraction Process

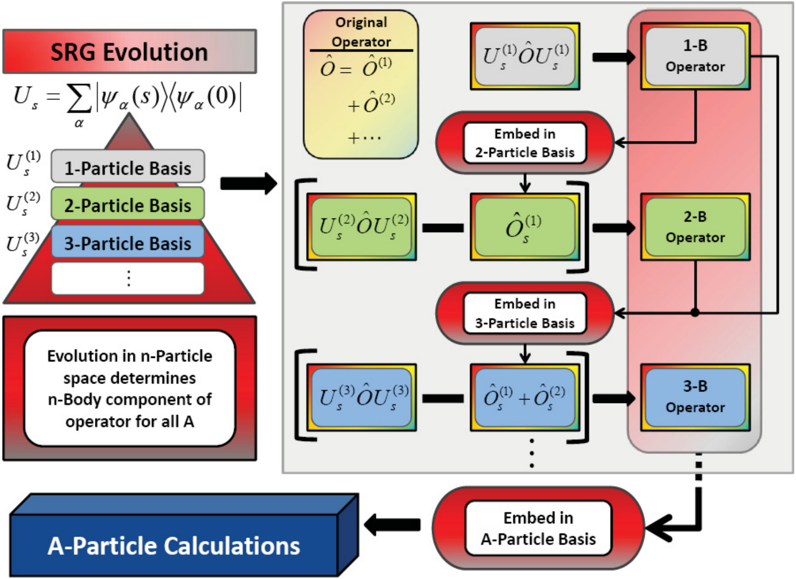

Operator Evolution & Extraction Process

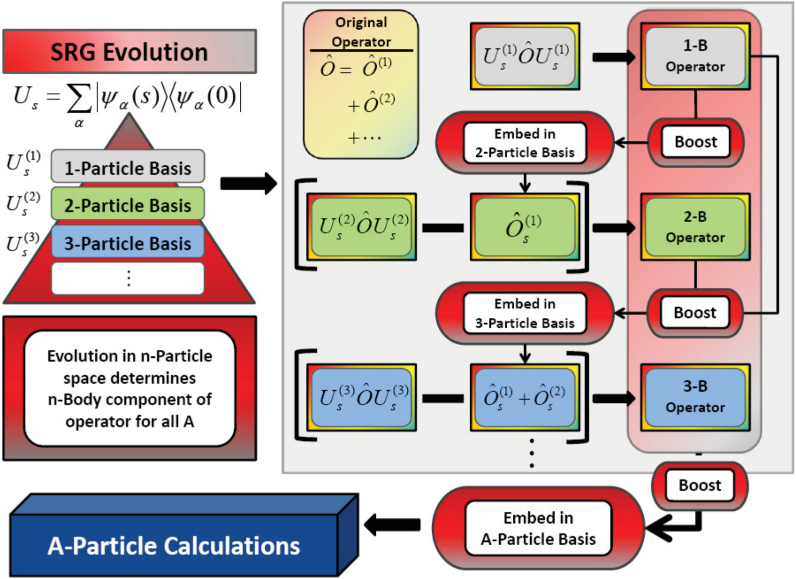

Relative Momentum Distribution: 1D Model

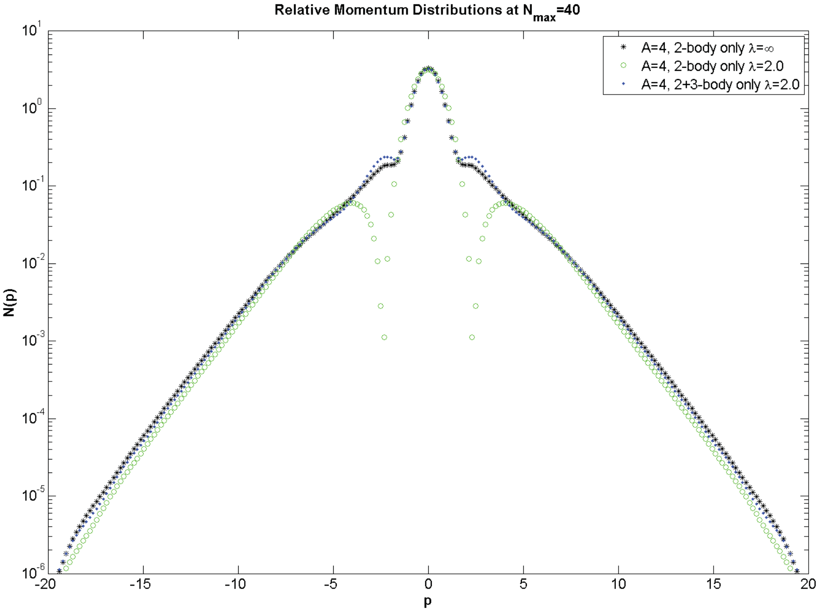

Single-Particle Momentum Distribution: 1D Model

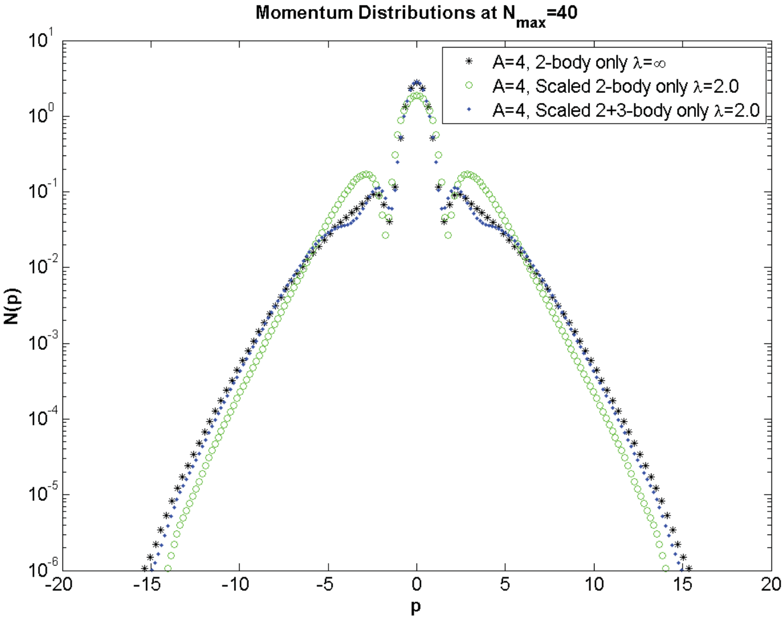

Electromagnetic Form Factors - 1-body Initial Current

- **Elastic electron-deuteron scattering**
- Calculation of G_C, G_Q, G_M operators at LO
- 1-body versus 2-body evolution?

  $\Longleftrightarrow$ bare versus evolved

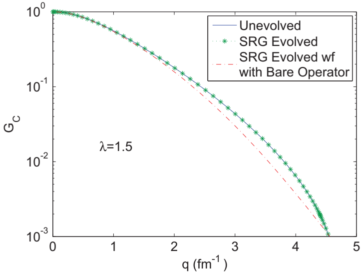

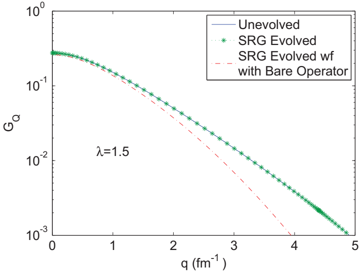

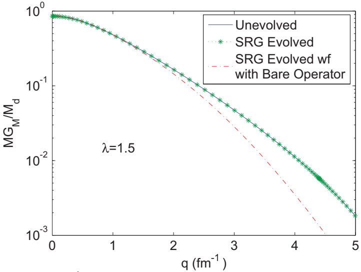

- Wave function is derived from the **NNLO 550/600 MeV – Epelbaum** *et al.* potential and the evolution is run to $\lambda = 1.5\,\mathbf{fm}^{-1}$.

Low Momentum Operators in NCSM

- **Evolve** Hamiltonian & operators **to** λ **at large** $N_{\max}$

  $\rightarrow$**Truncate** model space at N_{cut}

$$\Lambda_{UV} \sim \sqrt{mN_{max}\hbar\omega}; \quad \Lambda_{IR} \sim \sqrt{\frac{m\hbar\omega}{N_{max}}}$$

  $\rightarrow$ Poor convergence of long range operators . . . can this be corrected?

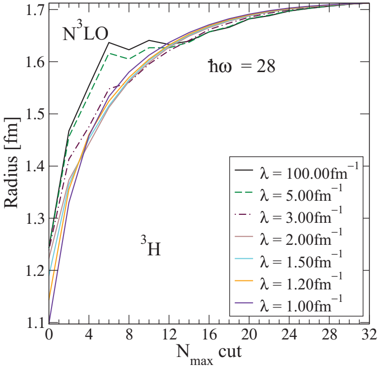

- SRG evolution of r^2 operator for A=3
  – Chiral N^{3}LO Potential with initial NN+NNN interaction
- **Stay tuned for many-body SRG evolution analysis of long- and short-distance operators!**

Controlled IR and UV renormalization

- Consider $T_{\rm rel} + \alpha r^2$, where α is a parameter which can be adjusted to optimize the renormalization (here, $\alpha = 10$), so that

$$\eta_s = [T_{\rm rel} + \alpha r^2, H_s]$$

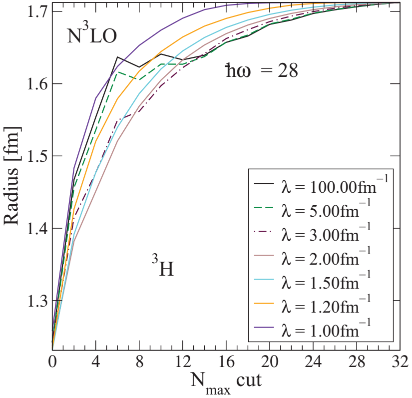

- Convergence improves with decreasing λ
- **Preliminary evidence:** spurious deep bound states appear in ^{4}He for small λ when embedding this H_s

Correlations in Nuclear Systems

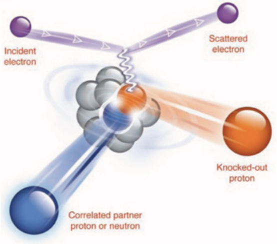

Subedi et al., Science 320,1476 (2008)

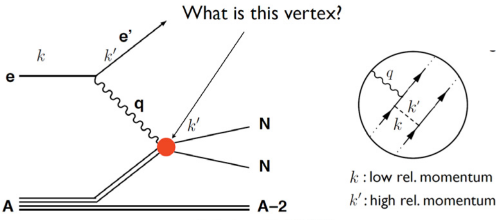

Higinbotham, arXiv:1010.4433

- E.g.: Detection of knocked out pairs with large relative momenta
- How is vertex modified?
- How to understand in context of SRG and low-momentum interactions?

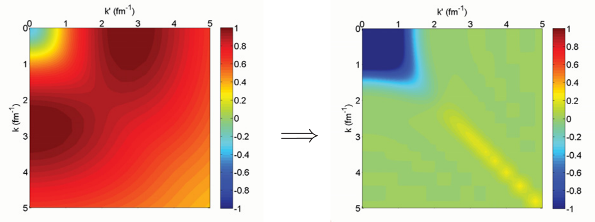

Nucleon Momentum Distributions

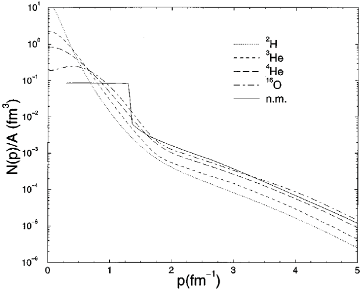

From Pieper, Wiringa, and Pandharipande (1992).

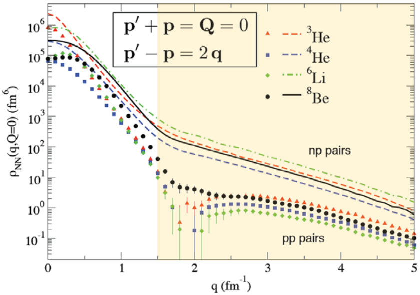

Schiavilla et al., PRL 98, 132501 (2007)

- Scaling behavior of momentum distribution function at large q

$$n_A(k) = a_2(A,d) \cdot n_d(k) \qquad \text{for } k > k_{Fermi}$$

– explained by dominance of NN potential & short-range correlations

- Dominance of *np* pairs over *pp* pairs: explained by tensor forces
- Hard interactions used (high resolution) . . . difficult calculations

Alternative: Calculation of pair density at low resolution . . .

→ Start with calculation of nuclear matter in MBPT:

Evolved Operators in Many-Body Perturbation Theory

Rewrite unitary transformation in 2nd quantization:

$$\widehat{U}_\lambda = 1 + \frac{1}{2}\left[U_\lambda\left(\frac{k_1-k_2}{2}, \frac{k_3-k_4}{2}\right) - \delta\left(\frac{k_1-k_2}{2}, \frac{k_3-k_4}{2}\right)\right]\delta\left(k_1+k_2, k_3+k_4\right) a^\dagger_{k_1} a^\dagger_{k_2} a_{k_4} a_{k_3} + \cdots$$

Example:

- Apply to 1-body operator for momentum distribution $\widehat{O} = a^\dagger_q a_q$:

$$\widehat{U}_\lambda \widehat{O} \widehat{U}^\dagger_\lambda \rightarrow a^\dagger_q a_q - a^\dagger_q a^\dagger_i a_i a_q + U_\lambda\left(\frac{k_1-k_2}{2}, \frac{i-q}{2}\right) a^\dagger_{k_1} a^\dagger_{k_2} a_{k_4} a_{k_3} U^\dagger_\lambda\left(\frac{i-q}{2}, \frac{k_3-k_4}{2}\right) + \cdots$$

- Apply to 2-body pair density operator $\widehat{O} = a^\dagger_{P/2+q} a^\dagger_{P/2-q} a_{P/2-q} a_{P/2+q}$:

$$\widehat{U}_\lambda \widehat{O}\, \widehat{U}^\dagger_\lambda =$$

$$U_\lambda\left(\frac{k_1-k_2}{2}, 2q\right) a^\dagger_{k_1} a^\dagger_{k_2} a_{k_4} a_{k_3} U^\dagger_\lambda\left(2q, \frac{k_3-k_4}{2}\right) + \cdots$$

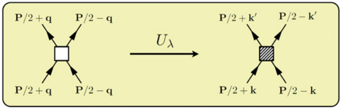

$\longrightarrow$ Implement perturbative expansion at small $\lambda = 1.8 - 3.0\,\text{fm}^{-1}$

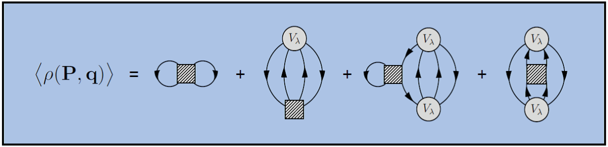

Work done with K. Hebeler

SRG Evolution of Operators in Nuclear Matter

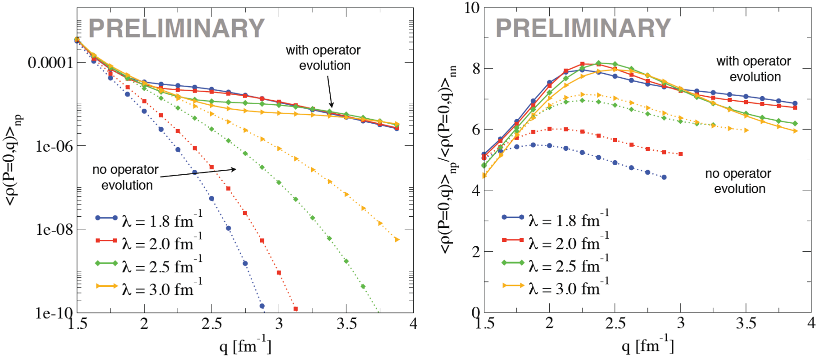

Using AV18 potential

- Pair-densities are approximately resolution independent
- Enhancement of *np* over *nn* pairs due to tensor force
- In progress: Calculation of a_2 in MBPT and HFB

Work done with K. Hebeler

SRG Evolution of Operators in Nuclear Matter

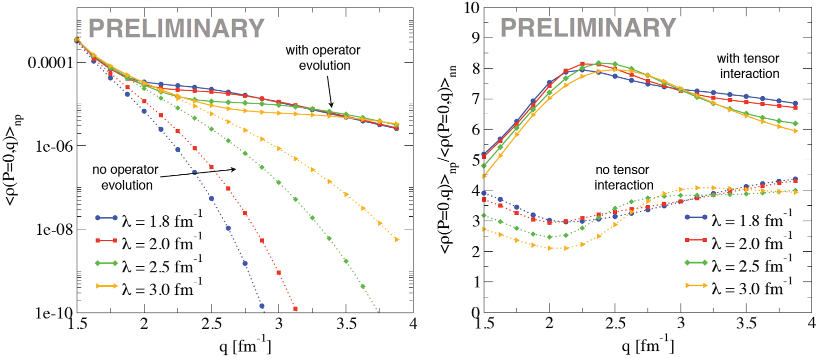

Using AV18 potential

- Pair-densities are approximately resolution independent
- Enhancement of *np* over *nn* pairs due to tensor force
- In progress: Calculation of a_2 in MBPT and HFB

Work done with K. Hebeler

Reproduction of Short-distance Physics

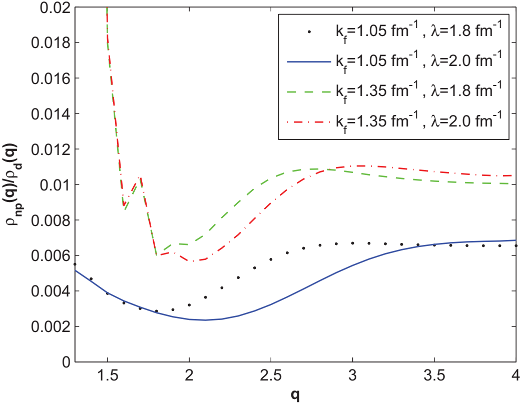

- Ratios of perturbative nuclear matter momentum distributions at densities of $k_f = 1.05\ \text{fm}^{-1}$ and $k_f = 1.35\ \text{fm}^{-1}$ for $\lambda = 1.8\ \text{fm}^{-1}$ and $\lambda = 2.0\,\text{fm}^{-1}$, as specified, over *ab-initio* calculation of the deuteron.
- Plateaus demonstrate the reproduction of high-momentum behavior in perturbative calculation of nuclear matter momentum distribution.
- Preliminary Calculation: proper normalization needed

Outline

Numerical Factorization in SRG

Idea: If $k < \lambda$ and $q \gg \lambda \Longrightarrow$ **factorization**: $U_\lambda(k,q) \to K_\lambda(k)Q_\lambda(q)$

- A **preliminary test of factorization** in U can be made by assuming

$$\frac{U_\lambda(k_i,q)}{U_\lambda(k_0,q)} \to \frac{K_\lambda(k_i)Q_\lambda(q)}{K_\lambda(k_0)Q_\lambda(q)},$$

so for $q \gg \lambda \Rightarrow \frac{K_\lambda(k_i)}{K_\lambda(k_0)}$, if $k < \lambda$.

- As shown below, one can infer this behavior from the plateaus for $q \gtrsim 2\text{fm}^{-1}$ when $k_i < \lambda$

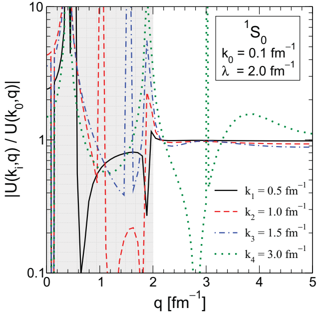

- **Singular Value Decomposition (SVD)**

  $\rightarrow$ tool to quantitatively analyze the extent to which U factorizes

  $\rightarrow$ The SVD can be expressed as an outer product expansion

$$G = \sum_i^r d_i \vec{u}_i \vec{v}_i^t$$

where r is the rank and the d_i are the singular values (in order of decreasing value).

- **Evidence**: Shown below at $\lambda = 2\,\text{fm}^{-1}$, for $q > \lambda$ and $k < \lambda$

	$^1S_0$		
Potential	$\mathbf{d_1}$	$\mathbf{d_2}$	$\mathbf{d_3}$
AV18	0.763	0.033	0.007
N3LO 500 MeV	1.423	0.221	0.015
N3LO 550/600 MeV	3.074	0.380	0.061
	$^3S_1$–$^3S_1$		
AV18	0.671	0.015	0.008
N3LO 500 MeV	1.873	0.225	0.044
N3LO 550/600 MeV	4.195	0.587	0.089

Factorization

- Motivation:

  The **Operator Product Expansion** (OPE) of the nonrelativistic wave function (Lepage)

$$\Psi_{true}(r) = \overline{\gamma}(r) \int d\mathbf{r}' \, \Psi_{eff} \delta_a(\mathbf{r}')$$

$$+ \overline{\eta}(r) a^2 \int d\mathbf{r}' \, \Psi_{eff} \nabla^2 \delta_a(\mathbf{r}') + \mathcal{O}(a^4)$$

  Similarly, in momentum space

$$\Psi_\alpha^\infty(q) \approx \gamma^\lambda(q) \int_0^\lambda p^2 dp \; Z(\lambda) \Psi_\alpha^\lambda(p)$$

$$+ \eta^\lambda(q) \int_0^\lambda p^2 dp \, p^2 \, Z(\lambda) \, \Psi_\alpha^\lambda(p)$$

  $\rightarrow \gamma^\lambda(q)$ and $\eta^\lambda(q)$ can be constructed by projecting the SRG evolved nuclear potential in momentum subspace to recover OPE via standard effective interaction methods

  Now, construct transformation directly:

$$U_\lambda(k,q) = \sum_\alpha \langle k|\psi_\alpha^\lambda\rangle \langle \psi_\alpha^\infty|q\rangle$$

$$\rightarrow \left[\sum_\alpha^{\alpha_{low}} \langle k|\psi_\alpha^\lambda\rangle \int_0^\lambda p^2 dp \; Z(\lambda) \Psi_\alpha^\lambda(p) \right] \gamma^\lambda(q)$$

$$\boxed{\Rightarrow U_\lambda(k,q) \approx \; K_\lambda(k) Q_\lambda(q)}$$

  If $k < \lambda$ and $q \gg \lambda \implies$ **factorization**

- Moreover, since $\psi_\alpha^\lambda(p)$ is suppressed for $p > \lambda$, we can extend the α sum to the full space and apply closure to find that $U_\lambda(k,q)$

$$\rightarrow \left[Z(\lambda) \int_0^\lambda d\widetilde{p} \sum_\alpha^\infty \left\langle k|\psi_\alpha^\lambda \right\rangle \left\langle \psi_\alpha^\lambda|p \right\rangle \right] \gamma^\lambda(q)$$

$$\approx Z(\lambda) \gamma^\lambda(q)$$

  Thus, the ratio $\frac{U_\lambda(k_i,q)}{U_\lambda(k_0,q)} \rightarrow 1$ to leading order in the factorization region . . . as seen in the previous slide!

Practical Use

- From **Decoupling**: write

$$\langle\psi_\lambda|\, U_\lambda \widehat{O}\, U_\lambda^\dagger\, |\psi_\lambda\rangle \cong$$

$$\int_0^\lambda dk' \int_0^\infty dq' \int_0^\infty dq \int_0^\lambda dk\; \psi_\lambda^\dagger(k') U_\lambda(k',q') \widehat{O}(q',q) U_\lambda(q,k) \psi_\lambda(k)$$

- Using **Factorization**: set $U_\lambda(k,q) \to K_\lambda(k) Q_\lambda(q)$, where $k < \lambda$ and $q \gg \lambda$.

$$\Longrightarrow \int_0^\lambda \int_0^\lambda \psi_\lambda^\dagger(k') \left[\int_0^\lambda \int_0^\lambda \underbrace{U_\lambda(k',q') \widehat{O}(q',q) U_\lambda(q,k)} + I_{QOQ} \underbrace{K_\lambda(k') K_\lambda(k)} \right] \psi_\lambda(k)$$

Low Momentum Structure

where $I_{QOQ} = \int_\lambda^\infty dq' \int_\lambda^\infty dq \left[Q_\lambda(q') \widehat{O}(q',q) Q_\lambda(q) \right]$ ← *Universal*

– *Valid* when initial operators *weakly couple high and low momentum*, e.g.,

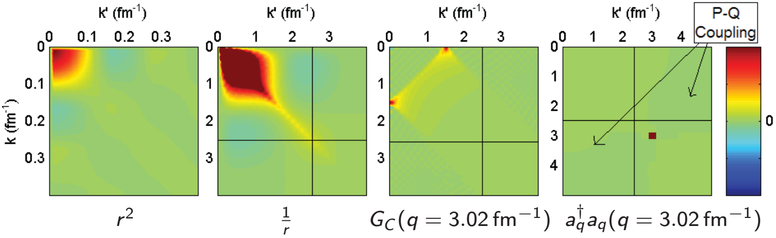

Factorization in Few-Body Nuclei

- **Variational Monte Carlo Calculation**
  → Using AV14 NN potential

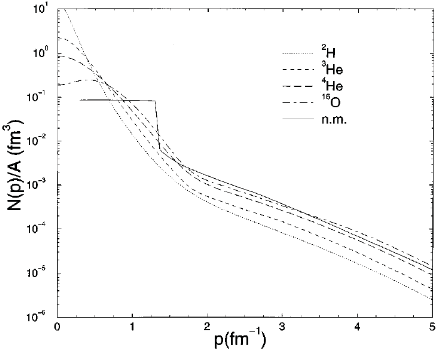

From Pieper, Wiringa, and Pandharipande (1992).

- Possible explanation of scaling behavior
  → Results from dominance of NN potential and short-range correlations (Frankfurt, et al.)

- **1D few-body HO space calculation**
  → System of A bosons interacting via a model potential

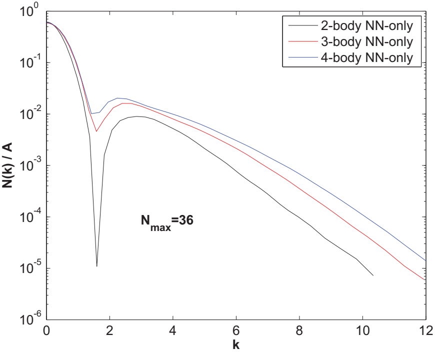

→ A Test Bed for 3D NCSM calculations:

- Alternative explanation of scaling behavior
  → Results from *factorization*

$$\int_0^\lambda \int_0^\lambda \psi_\lambda^\dagger(k')\,[I_{QOQ} K_\lambda(k') K_\lambda(k)]\,\psi_\lambda(k)$$

- **Variational Monte Carlo Calculation**
  → Using AV14 NN potential

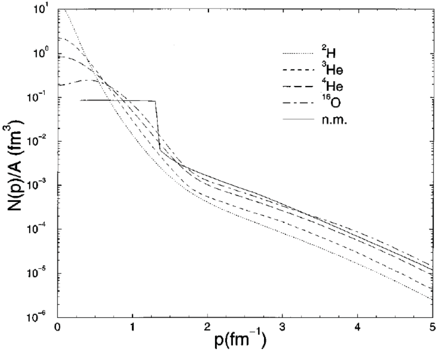

From Pieper, Wiringa, and Pandharipande (1992).

- Possible explanation of scaling behavior
  → Results from dominance of NN potential and short-range correlations (Frankfurt, et al.)

- **1D few-body HO space calculation**
  → System of A bosons interacting via a model potential

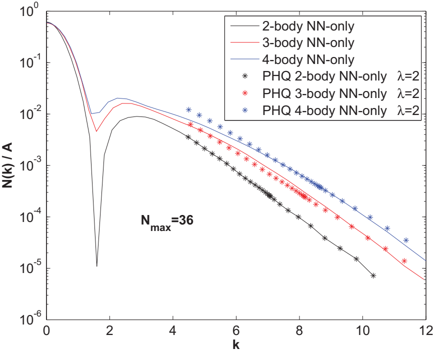

→ A Test Bed for 3D NCSM calculations:

- Alternative explanation of scaling behavior
  → Results from *factorization*

$$\int_0^{\lambda}\int_0^{\lambda} \psi_{\lambda}^{\dagger}(k')\,[I_{QOQ} K_{\lambda}(k') K_{\lambda}(k)]\,\psi_{\lambda}(k)$$

Long-distance 3-body contribution, etc.

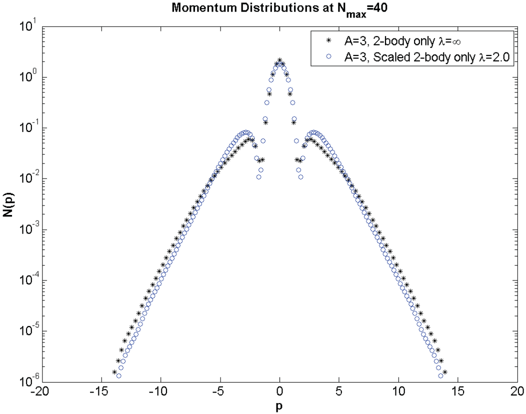

- Exact operator evolution and embedding: A=3 boson 1D model system momentum distributions
- Indication of factorization in many-particle space:

$$\left\{ \int_0^\lambda \int_0^\lambda \psi_\lambda^\dagger \left[K_\lambda(k') K_\lambda(k) \right] \psi_\lambda + \int_0^\lambda \int_0^\lambda \int_0^\lambda \int_0^\lambda \psi_\lambda^\dagger \left[K_\lambda(k_1', k_2') K_\lambda(k_1, k_2) \right] \psi_\lambda + \cdots \right\} I_{QOQ}$$

- In progress: Exploration of formal basis for n-body factorization

Long-distance 3-body contribution, etc.

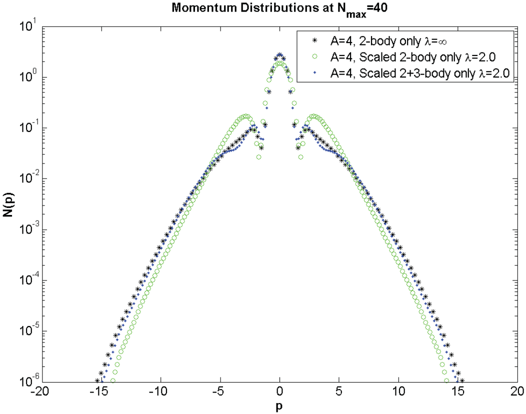

- Exact operator evolution and embedding: A=4 boson 1D model system momentum distributions
- Indication of factorization in many-particle space:

$$\left\{ \int_0^\lambda \int_0^\lambda \psi_\lambda^\dagger \left[K_\lambda(k') K_\lambda(k) \right] \psi_\lambda + \int_0^\lambda \int_0^\lambda \int_0^\lambda \int_0^\lambda \psi_\lambda^\dagger \left[K_\lambda(k_1', k_2') K_\lambda(k_1, k_2) \right] \psi_\lambda + \cdots \right\} I_{QOQ}$$

- In progress: Exploration of formal basis for n-body factorization

High-momentum tails from low-momentum ET's

S.K. Bogner & D. Roscher [arXiv:1208.1734]

Generalization of **factorization** to arbitrary A-body systems at low-momentum:

$$n(q) \approx Z_\Lambda^2 \gamma^2(\mathbf{q};\Lambda) \sum_{\mathbf{k},\mathbf{k}',\mathbf{K}} \langle \psi^\Lambda_{\alpha,A} | a^\dagger_{\frac{\mathbf{K}}{2}+\mathbf{k}} a^\dagger_{\frac{\mathbf{K}}{2}-\mathbf{k}} a_{\frac{\mathbf{K}}{2}+k'} a_{\frac{\mathbf{K}}{2}-\mathbf{k}'} | \psi^\Lambda_{\alpha,A} \rangle$$

– Can be shown for other operators

Example: Unitary Fermi gas

- Reproduction of contact Tan relation à la Braaten & Platter [2008]:

$$n(q) \approx \frac{Z_\Lambda^2 g^2(\Lambda)}{q^4} \sum_{\mathbf{k},\mathbf{k}',\mathbf{K}} \langle \psi^\Lambda_{\alpha,A} | a^\dagger_{\frac{\mathbf{K}}{2}+\mathbf{k}} a^\dagger_{\frac{\mathbf{K}}{2}-\mathbf{k}} a_{\frac{\mathbf{K}}{2}+k'} a_{\frac{\mathbf{K}}{2}-\mathbf{k}'} | \psi^\Lambda_{\alpha,A} \rangle = \frac{C(\Lambda_0)}{q^4}$$

- Static structure factor

$$S_{\uparrow\downarrow}(q) \approx -\left(\frac{2}{q^2 g(\Lambda)} + \frac{1}{8q} + \frac{\Lambda}{\pi^2 q^2}\right) Z_\Lambda^2 C(\Lambda) \longrightarrow \left(\frac{1}{8q} - \frac{1}{2\pi a q^2}\right) C(\Lambda_0)$$

$\longrightarrow$ Analogous relations reproduced for electron gas $\longleftarrow$

- Deep inelastic scattering ratio at $Q^2 \geq 2\,\text{GeV}^2$ and $0.35 \leq x_B \leq 0.7$ and inelastic scattering at $Q^2 \geq 1.4\,\text{GeV}^2$ and $1.5 \leq x_B \leq 2.0$
- Strong linear correlation between slope of ratio of DIS cross sections (nucleus A vs. deuterium) and nuclear scaling ratio
- SRG Factorization at leading order:
  $\rightarrow$ Dependence on high-q is *independent* of A
  $\rightarrow$ A-dependence from low momentum matrix element *independent* of operator

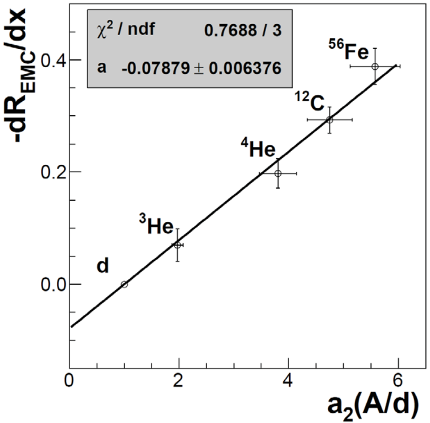

L.B. Weinstein, et al., Phys. Rev. Lett. 106, 052301 (2011)

- Why should A-dependence of nuclear scaling a_2 and the EMC effect be the same?

EFT approach to EMC Effect

Chen & Detmold [Phys. Lett. B 625, 165 (2005)]

The ratio relevant to the EMC effect is given by

$$R_A(x) = F_2^A(x)/AF_2^N(x) \quad \text{where the structure functions} \quad F_2^A = \sum_i Q_i^2 x q_i^A(x)$$

- In the EFT treatment: match leading-order nucleon operators to isoscalar twist-two quark operators

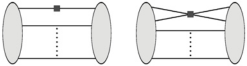

$$= \langle x^n \rangle_q \, v^{\mu_0} \cdots v^{\mu_0} N^\dagger N [1 + \alpha_n N^\dagger N] + \cdots$$

Implies: $R_A(x) = \frac{F_2^A(x)}{AF_2^N(x)} = 1 + g_{F2}(x)\mathcal{G}(A)$ where $\mathcal{G}(A) = \langle A|(N^\dagger N)^2|A\rangle / A\Lambda_0$

So, $\frac{dR_A}{dx}$ scales with $\mathcal{G}(A)$

- Connection to SRG Factorization:
  – Both imply factorization of long- and short-distance contributions

$$I_{QOQ} \iff g_{F2}(x)$$

$$\frac{\int_0^\lambda \int_0^\lambda \psi_\lambda^{A\dagger} [K_\lambda(k')K_\lambda(k)] \psi_\lambda^A}{\int_0^\lambda \int_0^\lambda \psi_\lambda^\dagger [K_\lambda(k')K_\lambda(k)] \psi_\lambda} \iff \mathcal{G}(A)$$

*** $[K_\lambda(k) \approx \text{constant}] \iff \delta(r) \iff \langle A|(N^\dagger N)^2|A\rangle$ ***

  – In Progress: quantitative calculation of A-dependence from SRG

Outline

Conclusions

Summary:

- SRG provides a means to lower the resolution needed in nuclear interactions, thereby reducing the computational difficulty of the nuclear many-body problem
- Many-body operators can be consistently evolved and extracted in SRG
- MBPT calculation of nuclear momentum distribution.
- Formal and numerical foundation for factorization of unitary transformation.
- Demonstration of factorization in many-body systems.
- Factorization greater understanding of separation of scales in nuclear systems
- A-dependence of nuclear scaling and the EMC effect from long-distance

Outlook:

- Quantitative calculation of nuclear scaling a_2 via factorization
  – MBPT with LDA
  – HFB
- Calculations in 3D in harmonic oscillator basis
- Explore other operators (e.g., electroweak) in 3D harmonic oscillator basis
  – utilize factorization
- Continue to explore generalization of factorization in 3-particle space
- Inclusion of higher-order effects via factorization

The End